

5. Turro, N. J. *Modern Molecular Photochemistry*; Benjamin/Cummings: Menlo Park, California, U.S.A., 1978; p 300.
6. Markham, J. J. *F-Centers in Alkali Halides*; Academic Press: New York, U.S.A., 1966; p 1.
7. Bosi, L.; Bussolati, C.; Spinolo, G. *Phys. Rev. B* **1970**, *1*, 890.
8. Dexter, D. L.; Klick, C. C.; Russell, G. A. *Phys. Rev.* **1955**, *100*, 603.
9. Gomes, L.; Morato, S. P. *J. Appl. Phys.* **1989**, *66*, 2754.
10. De Matteis, F.; Leblans, M.; Sloomans, W.; Schoemaker, D. *Phys. Rev. B* **1994**, 13186.
11. Gomes, L.; Luty, F. *Phys. Rev. B* **1984**, *30*, 7194.
12. Casalboni, M.; Proposito, P.; Grassano, U. M. *Solid State Commun.* **1993**, *87*, 305.
13. Yang, Y.; von der Osten, W.; Luty, F. *Phys. Rev. B* **1985**, *32*, 2724.
14. Halama, G.; Tsen, K. T.; Lin, S. H.; Luty, F.; Page, J. B. *Phys. Rev. B* **1989**, *39*, 13457.
15. Halama, G.; Tsen, K. T.; Lin, S. H.; Page, J. B. *Phys. Rev. B* **1991**, *44*, 2040.
16. Gustin, E.; Leblans, M.; Bouven, A.; Schoemaker, D. *Phys. Rev. B* **1996**, *54*, 6977.
17. Gustin, E.; Leblans, M.; Bouven, A.; Schoemaker, D. *Phys. Rev. B* **1996**, *54*, 6963.
18. Dierolf, V.; Luty, F. *Phys. Rev. B* **1996**, *54*, 6952.
19. Samiec, D.; Stolz, H.; von der Osten, W. *Phys. Rev. B* **1996**, *54*, 6977.
20. West, J.; Tsen, K. T. *Phys. Rev. B* **1994**, *50*, 9759.
21. Afanasiev, A.; Luty, F. *Solid State Commun.* **1996**, *98*, 531.
22. Lin, B. *Opt. Commun.* **1996**, *124*, 400.
23. Salminen, O.; Riihola, P.; Ozols, A.; Viitala, T. *Phys. Rev. B* **1996**, *53*, 6129.
24. An, C. P.; Luty, F. *Phys. Rev. B* **1997**, *56*, R5721.
25. Jang, D.-J.; Kelley, D. F. *Rev. Sci. Instrum.* **1985**, *56*, 2205.
26. Gomes, L.; Luty, F. *Phys. Rev. B* **1995**, *52*, 7094.
27. Kittel, C. *Introduction to Solid State Physics*; John Wiley & Sons: New York, U.S.A., 1976; p 21.
28. Mollenauer, L. F.; Baldacchini, G. *Phys. Rev. Lett.* **1972**, *29*, 465.
29. Klein, M. V.; Wedding, B.; Levine, M. A. *Phys. Rev. B* **1969**, *180*, 902.
30. Kapphan, S.; Luty, F. *Solid State Commun.* **1970**, *8*, 349.
31. Holstein, T.; Lyo, S. K.; Orbach, R. *Phys. Rev. B* **1977**, *6*, 934.
32. Inokuti, M.; Hirayama, F. *J. Chem. Phys.* **1965**, *43*, 1978.
33. Dexter, D. L. *J. Chem. Phys.* **1953**, *21*, 836.
34. Klafter, J.; Blumen, A. *J. Lumin.* **1985**, *34*, 77.
35. Yang, C.-L.; El-Sayed, M. A. *J. Phys. Chem.* **1986**, *90*, 5720.
36. Mario, H. J.; McGlynn, S. P. *J. Chem. Phys.* **1970**, *52*, 3402.

Molecular Dynamics Simulation Study on Segmental Motion in Liquid Normal Butane

Song Hi Lee* and Han Soo Kim†

Department of Chemistry, Kyungsoong University, Pusan 608-736, Korea

†Department of Industrial Chemistry, Kangnung National University, Kangnung 212-702, Korea

Received June 13, 1998

We present results of molecular dynamic (MD) simulations for the segmental motion of liquid *n*-butane as the base case for a consistent study for conformational transition from one rotational isomeric state to another in long chains of liquid *n*-alkanes. The behavior of the hazard plots for *n*-butane obtained from our MD simulations are compared with that for *n*-butane of Brownian dynamics study. The MD results for the conformational transition of *n*-butane by a Poisson process from the total first passage times are different from those from the separate *t*→*g* and *g*→*t* first passage times. This poor agreement is probably due to the failure of the detailed balance between the fractions of *trans* and *gauche*. The enhancement of the transitions *t*→*g* and *g*→*t* at short time regions are also discussed.

Introduction

In recent papers,¹⁻³ we carried out equilibrium molecular dynamics simulations of three different models for liquid alkanes to investigate the thermodynamic, structural, and dynamic properties of liquid normal alkanes (*n*-butane to *n*-heptadecane) and branched alkanes (isobutane, 4-propyl heptane, 6-pentyl dodecane, and 5-dibutyl nonane). In the

present paper the same technique is applied to study the segmental motion of normal butane as the base case for a consistent study of conformational transitions from one rotational isomeric state to another in long chains of liquid *n*-alkanes.

In recent years, there has been considerable experimental and theoretical interest in the dynamics of molecular conformational motion in solution. Computer simulation of

the structural formation of polymer chains has become the focus of attention in physics, chemistry, and material science. Intensive studies of various model polymer systems⁴⁻⁹ have been made in order to understand the dynamics of conformational transitions. Recent experimental advances in laser spectroscopy make it possible to follow directly ultrafast processes with isomerization rates in the pico- or subpicosecond domain. Unfortunately such optical detection usually requires labeling with chromophore groups that may modify the dynamical properties severely. Nuclear magnetic resonance (NMR) coupled relaxation experiments¹⁰⁻¹⁵ in multispin systems also provide a powerful method for probing local as well as overall rotational dynamics in solution. Furthermore, these NMR methods at most only require the isotopic substitution of ¹³C for ¹²C or ²H for ¹H.

However, these experiments may not reveal many of the details about the motion, such as whether correlation exist between transitions of near neighbors, or, in general, what the effect of the rest of the chain is on the bond undergoing transitions. That the rest of the chain, or the tails, plays some role is evident. Clearly, as a particular bond rotates, the attached tails cannot rigidly follow without experiencing a large frictional resistance.

When one bond in a long chain of a polymer in solution undergoes a conformational transition, if there is no accompanying transition of any bonds of the tails, the tails' positions in space after the transition differ markedly from the initial positions. The bond undergoes a large rotational displacement which induces a large solvent frictional resistance. There are certain modes of motion (so-called crankshaft), such as the Schatzki crankshaft¹⁶ or the three-body motion,¹⁷ which leave the tails in the same position at the start and end of the transition. Such motions involve two barrier crossings, or the passage through some fairly high energy intermediate state.

The question arises as to what the differences are between the processes of conformational transitions in small molecules and in polymers. The rate of such conformational changes in a small molecule can be calculated by standard reaction rate theory. An implicit assumption is that on the time scale of transitions the modes of motion orthogonal to the reaction coordinate have ample time to maintain a local equilibrium. This cannot be the case for polymers. Intuitively we can see that for many conformational changes the long polymer tails attached to the rotating bond would have to swing around, which would be resisted by a large frictional resistance.

In the present paper, conformational transitions have been looked at in open *n*-butane chain which has only one dihedral state. The conformational motion here is just the motion of the attached methyl group with fixed three centers of the other methyl and methylene groups in a molecule. We consider neither cooperative transition nor crankshaft. As the simplest case of conformational transitions, the torsional rotational dynamics of *n*-butane chain would provide a valuable fundamental information for segmental motions in a short chain. The paper is organized as follows. Section II contains a brief description of molecular models and molecular dynamics (MD) simulation methods followed by Section III which presents the results of our simulations and Section IV where our conclusions

are summarized.

Molecular Model and Molecular Dynamics Simulations

In the present study, we have carried out for MD simulations of liquid *n*-butane at various temperatures using an expanded collapsed atomic model.¹⁸⁻²⁰ Each simulation was carried out in the NVT ensemble; the density and hence the length of cubic simulation box were fixed ($N=64$ and $\rho=0.583$ g/cc). The usual periodic boundary condition in the *x*-, *y*-, and *z*-directions and minimum image convention for pair potential were applied. A spherical cut-off of radius $R_c=2.5 \sigma$, where is the LJ parameter, was employed for all the pair interactions. Gaussian isokinetics^{21,22} was used to keep the temperature of the system constant.

The molecular model adopted for *n*-butane is so called the expanded collapsed atomic model. Monomeric units are treated as single spheres with masses of 14.531 g/mole. They interact through an LJ potential between the spheres in different molecules and between the spheres more than three apart on the same molecule. The C-C-C-C torsional rotational potential is given by the original Ryckaert-Bellemans form²³:

$$V(\phi) = c_0 + c_1 \cos \phi + c_2 \cos^2 \phi + c_3 \cos^3 \phi + c_4 \cos^4 \phi + c_5 \cos^5 \phi \quad (1)$$

where ϕ is the C-C-C-C dihedral angle. The LJ parameters and c_i 's are listed in Table 1. There are actually five independent constants in this potential, which may be specified: the height of the *trans-gauche* barrier, $E_g^* = 12.340$ kJ/mole; the energy difference between the *trans* and *gauche* minima, $E_g = 2.938$ kJ/mole (and $E_g^* = 9.402$ kJ/mole); the energy at the *cis* state, $E_{cis} = 44.818$ kJ/mole; the angular location of the barrier, $\phi^* = \pm 60^\circ$; and the angular location of the *gauche* minimum, $\phi_g = \pm 120^\circ$.

This model also includes the C-C bond stretching and C-C-C bond angle bending potentials in addition to the LJ and torsional potentials of the above Ryckaert-Bellemans potential:

$$V_b(r_{ij}) = K_0(r_{ij} - r_e)^2 \quad (2)$$

$$V_a(\theta) = K_1(\theta - \theta_e)^2 - K_2(\theta - \theta_e)^3 \quad (3)$$

The equilibrium bond length (r_e) and bond angle (θ_e), and the force constants (K_0 , K_1 , and K_2) are used by Chynoweth *et al.*¹⁸⁻²⁰ which are originally provided by the work of White and Boville,²⁴ and are given in Table 1.

For the integration over time, we adopted Gear's fifth-

Table 1. Potential parameters for liquid *n*-butane

LJ parameters	σ (nm)	ϵ (kJ/mol)				
C-C	0.3923	0.5986				
torsional	c_0 (kJ/	c_1	c_2	c_3	c_4	c_5
C-C-C-C	9.279	12.136	-13.120	-3.060	26.240	-31.495
bond stretching	r_e (nm)	K_0 (kJ/mol·nm ²)				
C-C	0.153	132600				
bond angle bending	θ_e (deg)	K_1 (kJ/mol·deg ²)	K_2 (kJ/mol·deg ³)			
C-C-C	109.47	0.05021	0.000482			

order predictor-corrector algorithm²⁵ with a time step of 0.0005 ps. A total of 12,000,000 time steps was simulated each for the average and the configurations of molecules were stored every 10 time steps for further analysis.

Conformational Transition of *n*-butane

The dihedral angle ϕ for a given C-C bond is one of the three states - *gauche*-plus (g^+), *trans* (t), or *gauche*-minus (g^-) by the C-C-C-C torsional rotational potential. When ϕ arrives at the minimum of one of the potential wells, we set a clock equal to zero and count the number of time steps required for the bond to first reach the minimum of the other wells. Then we reset the clock zero and measure the next transition time, etc. The transition times are the first passage times from one minimum to the other. Thus there is obtained a set of n transition times. These are arranged in ascending order, $t_{(1)} \leq t_{(2)} \leq \dots \leq t_{(n)}$, forming what is called a set of order statistics.

The information contained in the set of first passage times is best depicted in a hazard plot. Let $h(t)$, the hazard rate, be defined such that $h(t)dt$ is the probability that a bond, which has not had a transition in a time t since the last transition, has a transition between t and $t+dt$. Define the cumulative hazard as

$$H(t) = \int_0^t h(t') dt'. \quad (4)$$

It is easily shown that the probability, $P(t)$, that a bond has the next transition in a time less than t since the last transition is related to the hazard by

$$P(t) = 1 - \exp[-H(t)] \quad (5)$$

and the probability density of a transition at t is

$$p(t) = dP/dt = h(t)\exp[-H(t)]. \quad (6)$$

In Figure 1 we plot hazard plots for *n*-butane molecular dynamics simulations at various temperatures of 293, 263, 233, and 203 K. The plots are straight lines except in the short time regions. The rate measured is a composite of all

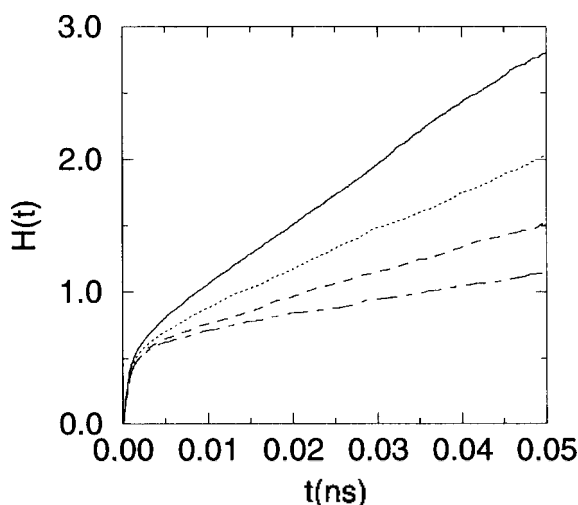


Figure 1. Hazard plots for *n*-butane molecular dynamics simulations at 293 (—), 263 (···), 233 (---), and 203 K (-·-·-) obtained from the total first passage times.

processes, *trans* going to either one of the *gauches* or vice versa:

$$\lambda = 2p_t \lambda_{tg} + 2p_g \lambda_{gt}. \quad (7)$$

where λ_{tg} is the rate of transition from *trans* to one of the *gauches*, λ_{gt} is the reverse rate, p_t is the fraction of *trans*, and p_g is the fraction of one of the *gauche* states. Detailed balance requires that

$$p_t \lambda_{tg} = p_g \lambda_{gt}. \quad (8)$$

so that

$$\lambda_{tg} = \lambda/(4p_t). \quad (9)$$

The behavior of hazard plots for *n*-butane obtained from our MD simulation is different from that for *n*-butane of Brownian dynamics (BD) study⁵: the hazard plot from MD at 298 K shows an enhanced transition at short time (≤ 0.03 ps) and then almost a straight line with a slope of $\lambda=45.0$ ns⁻¹ while the hazard plot from BD at 425 K is nearly a straight line for the whole time region with a slope of $\lambda=67.1$ ns⁻¹. Rather, this behavior is very similar to that of polymer conformation transition in the same BD study.⁵ The slopes in the short time regions of Figure 1 are higher, indicating a higher rate of transition. Since small t means short times since the last transition, the higher slope indicates that immediately after one transition occurs there is an enhanced rate for another transition. The major reason for the enhanced short time transition rate in the polymer conformation may appear to be that when a transition occurs the neighbors may not be in, or relax into, a position which can accept this new conformation. However, in the case of *n*-butane, there is no neighbor atom in the same molecule but neighbor atoms in different molecules in our MD simulation. If the first transition was $t \rightarrow g^\pm$, the second is almost always the reverse since the *cis* barrier is quite high. But $g^\pm \rightarrow t$ can be followed either the reverse or by $t \rightarrow g^\pm$. The fractions for which the first state is *gauche* and goes back to the same *gauche* are 40.2, 40.5, 38.6, and 37.4% at 203, 233, 263 and 293 K, respectively. This results is much different from 90.6% of $g^\pm \rightarrow t \rightarrow g^\pm$ at 372 K in the explanation for the enhanced short time transition rate in the polymer conformation transition of Brownian dynamics study.⁵

There is no enhanced transition at short time region in the hazard plot for *n*-butane of Brownian dynamics (BD) study.⁵ The main reason for this difference may come from the difference in the methods of computer simulations—molecular dynamics (MD) and Brownian dynamics (BD). The equations which describe Brownian motion are the Langevin equations in which the force of frictional resistance is taken as being equal to in magnitude and opposite in direction to the sum of the potential force and the Brownian random force. The total potential is a sum of the intramolecular potentials, Eqs. (1)-(3), considering only one *n*-butane molecule. The random force is Gaussianly distributed with mean zero and some magnitude of covariance.⁵ But in our molecular dynamics (MD) simulation of pure liquid *n*-butane, there are intermolecular interactions between 64 *n*-butane molecules instead of the random force in addition to the intramolecular potentials. The main difference in methodology between MD and BD

is the treatment of forces exerted by solvent molecules. There are no solvent molecules in our MD simulation of *n*-butane.

In describing the hazard curve, many analytical approximations are possible. We consider only that all the uncompleted reactions which reverse are regarded as reversing instantly and that thereafter the transitions to new states are a Poisson process with rate λ_n . In that case the hazard rate is

$$h(t) = \lambda_o + v_o \delta(t-) \quad (10)$$

and the cumulative hazard is

$$H(t) = \lambda_o t + v_o. \quad (11)$$

According to Eq. (5), the probability of a transition having occurred in a time less than t is

$$P(t) = 1 - (1 - c_o) \exp[-\lambda_o t], \quad t > 0 \quad (12)$$

$$c_o = 1 - \exp[-v_o]. \quad (13)$$

From the fact that $P(0+) = c_o$, we can identify c_o as the fraction of "transitions" that immediately reverse. A measure of c_o can be obtained by fitting the asymptotic portion of the hazard plot with a straight line and using the intercept, v_o , in Eq. (13). The fit has been done by least squares, omitting the data in the short time, severely nonlinear region. The calculated c_o 's are listed in Table 2.

The results are reported in Table 2 where the rates λ are calculated from the hazard fit to Eq. (11) by least squares, excluding the short time regions, λ_{tg} and λ_{gt} are obtained from Eqs. (8) and (9). The transition rates $\lambda_{\alpha\beta}$ are given in the form of a prefactor $f_{\alpha\beta}$ and an activation energy $E_{\alpha\beta}^+$ defined by

Table 2. Transition rates for *n*-butane at various temperatures

T(K)	λ	λ_{tg}	λ_{gt}	p_t	$c_o(\%)$	λ_{tg}	$c_o(\%)$	λ_{gt}	$c_o(\%)$	p_t
293	45.0	17.9	60.6	0.629	45.8	17.2	46.6	67.4	34.3	0.662
263	28.5	10.8	41.6	0.658	45.4	10.2	47.8	41.4	38.6	0.670
233	18.8	6.73	30.9	0.697	44.2	6.03	47.0	30.9	39.3	0.719
203	10.6	3.51	21.2	0.751	46.2	2.62	50.9	15.0	38.2	0.741

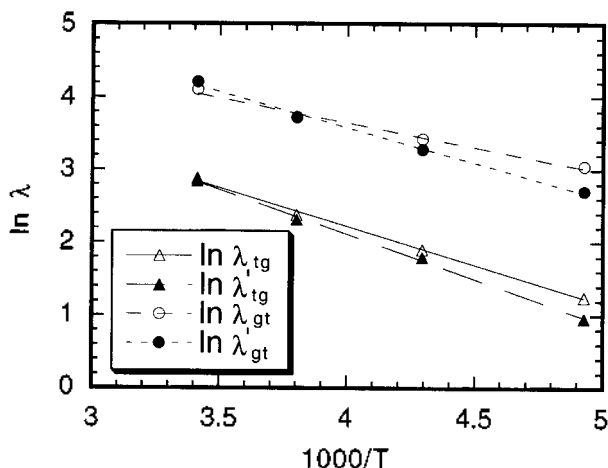


Figure 2. Arrhenius plots of the logarithm of the transition rates vs. $1000/T$.

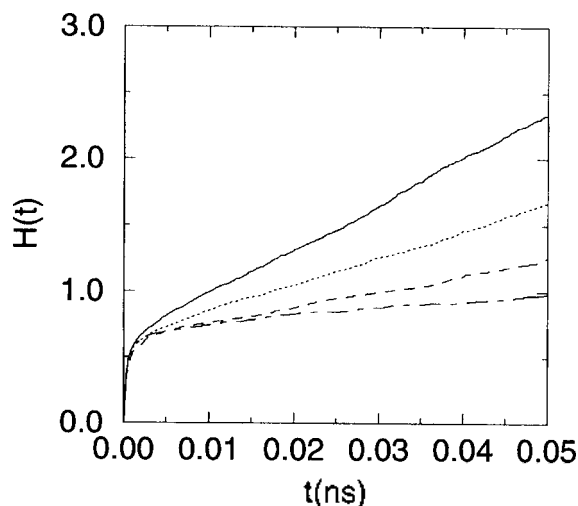


Figure 3. Hazard plots for *n*-butane molecular dynamics simulations at 293 (—), 263 (···), 233 (---), and 203 K (-·-·-) obtained from the $t \rightarrow g$ first passage times.

$$\lambda_{\alpha\beta} = f_{\alpha\beta} \exp(-E_{\alpha\beta}^+/kT). \quad (14)$$

An Arrhenius plot of the transition rates from Table 2, Figure 2, gives activation energies of $E_{tg}^+ \approx 0.714 E_{ig}^*$ with $f_{tg} = 640 \text{ ns}^{-1}$ and $E_{gt}^+ \approx 0.600 E_{gt}^*$ with $f_{gt} = 582 \text{ ns}^{-1}$.

Instead of using Eqs. (7)-(9), we divided the total first passage times into two parts according to the first state of the bond: the $t \rightarrow g$ and $g \rightarrow t$ first passage times. The calculated hazard plots from these first passage times at 293, 263, 233, and 203 K are plotted in Figures 3 and 4. The rates λ'_{tg} and λ'_{gt} are obtained from the hazard fit to Eq. (11) by least squares, excluding the short time regions and listed in Table 2. These results for $\lambda'_{\alpha\beta}$ are not much different from those for from the total first passage time. But the calculated activation energies by Eq. (14) are very different, which are $E_{tg}^+ \approx 0.827 E_{ig}^*$ with $f_{tg} = 1119 \text{ ns}^{-1}$ and $E_{gt}^+ \approx 0.862 E_{gt}^*$ with $f_{gt} = 1784 \text{ ns}^{-1}$. The failure of complete agreement between these two transition rates from the total first passage times and the $t \rightarrow g$ and $g \rightarrow t$ first passage times

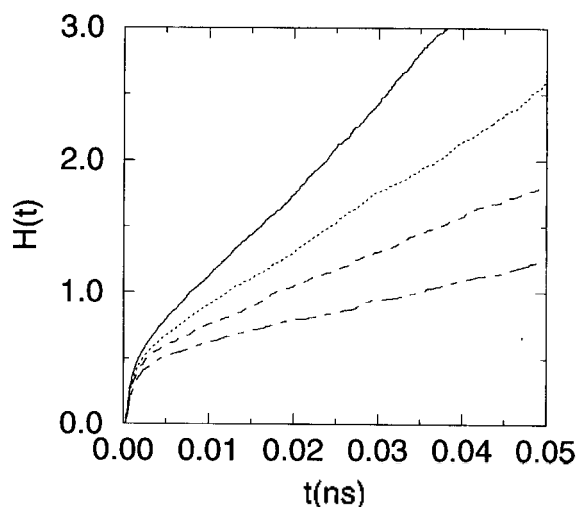


Figure 4. Hazard plots for *n*-butane molecular dynamics simulations at 293 (—), 263 (···), 233 (---), and 203 K (-·-·-) obtained from the $g \rightarrow t$ first passage times.

is due to the detailed balance between the fractions of *trans* and *gauche*. Using the detailed balance, Eq. (8), and the relationship between the fraction of *trans* and the fraction of one of the *gauche* states, $1=p_t+2p_g$, the calculated fractions of *trans* at various temperatures are obtained and given in the last column of Table 2. The difference in p_t and p_g reflects the difference in $\lambda_{\alpha\beta}$ and $\lambda_{\alpha\beta}^1$.

The enhancement of the transition $t \rightarrow g$ at short time regions is larger than that of the $g \rightarrow t$ as seen in the fraction of immediately reversing transitions, c_{ir} , in Table 2. Why the immediately reversing transition of the $t \rightarrow g$ is larger than that of the $g \rightarrow t$ even the barrier height of $t \rightarrow g$ is higher than that of $g \rightarrow t$? One possible explanation is as follows: the previous transition of $t \rightarrow g$ is either $g^+ \rightarrow t$ or $g^- \rightarrow t$ and as discussed above the fraction of the consecutive transition $g^- \rightarrow t \rightarrow g^+$ is 37.4% at 293 K and the $g^- \rightarrow t \rightarrow g^+$ 62.6%. Since the conformational transitions of *n*-butane in MD simulation is due to the intermolecular interaction and the torsional rotational motion is more likely to continue ($g^+ \rightarrow t \rightarrow g^-$) than to change the direction ($g^+ \rightarrow t \rightarrow g^+$). Similarly the previous transition $g \rightarrow t$ is $t \rightarrow g$. Since the *cis* potential is too high for the transition $g^+ \rightarrow g^-$ or $g^- \rightarrow g^+$ (we have never observed a *cis* barrier crossing), the consecutive $t \rightarrow g \rightarrow t$ is to change the direction of the torsional rotational motion and hence the immediately reversing transition $g \rightarrow t$ is not more favorable than the $t \rightarrow g$.

Conclusion

We have carried out molecular dynamics (MD) simulations to investigate the conformational transition of liquid *n*-butane at various temperatures. The behavior of the hazard plots for *n*-butane obtained from our MD simulation, characterized by the enhancement of transition at short time regions, is completely different from that for *n*-butane of Brownian dynamics study.⁵ The MD results for the conformational transition of *n*-butane by a Poisson process from the total first passage times are compared with those from the separate $t \rightarrow g$ and $g \rightarrow t$ first passage times. This poor agreement is probably due to the failure of the detailed balance between the fractions of *trans* and *gauche*. The enhancement of the transitions $t \rightarrow g$ and $g \rightarrow t$ at short time regions are discussed. The conformational transition of a long chain of *n*-heptadecane is under study.

Acknowledgment. This research was supported by Kyungsoong University Research Grants in 1997 to SHL. SHL thanks the Korea Institute of Sciences and Technology for access to the Cray-C90 super computer and the Tongmyung University of Information Technology for access to its IBM SP/2 computers.

References

1. Lee, S. H.; Lee, H.; Pak, H.; Rasajiah, J. C. *Bull. Kor. Chem. Soc.* **1996**, *17*, 735.
2. Lee, S. H.; Lee, H.; Pak, H. *Bull. Kor. Chem. Soc.* **1997**, *18*, 478.
3. Lee, S. H.; Lee, H.; Pak, H. *Bull. Kor. Chem. Soc.* **1997**, *18*, 501.
4. Helfand, E.; Skolnick, J. J. *J. Chem. Phys.* **1982**, *77*, 5714.
5. Helfand, E.; Wasserman, E. R.; Weber, T. A. *Macromolecules* **1980**, *13*, 526.
6. Helfand, E. *Science* **1984**, *226*, 647.
7. Pastor, R. W.; Venable, R. M.; Karplus, M. *J. Chem. Phys.* **1988**, *89*, 112.
8. Pastor, R. W.; Venable, R. M.; Karplus, M.; Szabo, A. *J. Chem. Phys.* **1988**, *89*, 1128.
9. Levy, R. M.; Karplus, M.; Wolynes, P. G. *J. Am. Chem. Soc.* **1981**, *103*, 5998.
10. Mayne, C. L.; Alderman, D. W.; Grant, D. M. *J. Chem. Phys.* **1975**, *63*, 2514.
11. Mayne, C. L.; Grant, D. M.; Alderman, D. W. *J. Chem. Phys.* **1976**, *65*, 1684.
12. Courtieu, J.; Gonord, P.; Mayne, C. L. *J. Chem. Phys.* **1980**, *72*, 953.
13. Brown, M. S.; Grant, D. M. Horton, W. J.; Mayne, C. L.; Evans, G. T. *J. Am. Chem. Soc.* **1985**, *107*, 6698.
14. Liu, F.; Mayne, C. L.; Grant, D. M. *J. Mag. Reson.* **1989**, *84*, 344.
15. Fuson, M. M.; Grant, D. M. *Macromolecules* **1988**, *21*, 949.
16. Schatzki, T. F. *J. Polym. Sci.* **1962**, *57*, 496.
17. Monnerie, L.; Geny, F. *J. Chem. Phys.* **1969**, *66*, 1691.
18. Chynoweth, S.; Klomp, U. C.; Scales, L. E. *Comput. Phys. Commun.* **1991**, *62*, 297.
19. Chynoweth, S.; Klomp, U. C.; Michopoulos, Y. *J. Chem. Phys.* **1991**, *95*, 3024.
20. Berker, A.; Chynoweth, S.; Klomp, U. C.; Michopoulos, Y. *J. Chem. Soc. Faraday Trans.* **1992**, *88*, 1719.
21. Evans, D. J.; Hoover, W. G.; Failor, B. H.; Moran, B.; Ladd, A. J. C. *Phys. Rev.* **1983**, *A28*, 1016.
22. Simmons, A. D.; Cummings, P. T. *Chem. Phys. Lett.* **1986**, *129*, 92.
23. Ryckaert, J. P.; Bellemans, A. *Discuss. Faraday Soc.* **1978**, *66*, 95.
24. White, D. N. J.; Boville, M. J. *J. Chem. Soc., Perkin Trans.* **1977**, *2*, 1610.
25. Gear, C. W. *Numerical Initial Value Problems in Ordinary Differential Equation*; Englewood Cliffs NJ; Prentice-Hall, 1971.